

聚丙烯腈基碳纤维对比分析:(一)微观结构

李登华¹, 吕春祥², 郝俊杰³, 王惠民⁴

(1. 山西省交通科技研发有限公司 新型道路材料国家地方联合工程实验室, 山西 太原 030032;

2. 中国科学院山西煤炭化学研究所 碳纤维制备技术国家工程实验室, 山西 太原 030001;

3. 山西钢科碳材料有限公司, 山西 太原 030100;

4. 华东理工大学 化工学院, 上海 200237)

摘要: 利用X射线广角衍射/小角散射、Raman光谱及高分辨透射显微镜对不同型号聚丙烯腈基碳纤维的晶态结构、孔结构、径向结构不均匀性、石墨化度、内部残余应力、结构取向性及分形现象进行了对比分析。结果表明, MJ碳纤维的微晶结构比T系列提升明显, 内部残余应力逐步释放, 结构取向性显著提升, 石墨化程度也显著增强; 但其微孔尺寸有所增大, 径向结构不均匀性增加, 体现了石墨化过程对碳纤维微观结构的显著影响。

关键词: 碳纤维; 晶态结构; 石墨化度; 结构不均匀性; 分形

中图分类号: TQ342+.74

文献标识码: A

基金项目: 山西省重点研发计划项目(201903D121005); 山西交通控股集团有限公司科技项目(18-JKKJ-22, 19-JKKJ-53); 山西省科技重大专项(20181101019)。

通讯作者: 李登华, 博士, 高级工程师. E-mail: yob2846@163.com

A comparative analysis of polyacrylonitrile-based carbon fibers: (I) Microstructures

LI Deng-hua¹, LU Chun-xiang², HAO Jun-jie³, WANG Hui-min⁴

(1. National and Local Joint Engineering Laboratory of Advanced Road Materials, Shanxi Transportation Technology Research & Development Co., Ltd, Taiyuan 030032, China;

2. National Engineering Laboratory for Carbon Fiber Technology, Institute of Coal Chemistry, Chinese Academy of Sciences, Taiyuan 030001, China;

3. Shanxi Gangke Carbon materials Co., Ltd, Taiyuan 030100, China;

4. School of Chemical Engineering, East China University of Science and Technology, Shanghai 200237, China)

Abstract: X-ray wide angle diffraction/small angle scattering, Raman spectroscopy and high resolution transmission electron microscopy were used to characterize the crystalline structure, pore structure, radial structural heterogeneity, degree of graphitization, internal residual stress, crystalline orientation and fractal phenomena of various grades (T and MJ) of polyacrylonitrile-based carbon fibers made by Toray Inc, Japan. Results showed that compared with the T series fibers, the MJ series fibers had a significantly lower internal residual stress, better structural orientation and a much higher degree of graphitization, but the dimensions of the microvoids and the radial inhomogeneity were increased, which revealed the significant influence of graphitization conditions in making MJ series fibers on the microstructures of carbon fibers.

Key words: Carbon fiber; Crystalline structure; Degree of graphitization; Structural heterogeneity; Fractal

Received date: 2020-03-26; *Revised date:* 2020-07-16

Foundation item: Key Research and Development (R&D) Projects of Shanxi Province (201903D121005); Project of Shanxi Transportation Holdings Group Co. Ltd. (18-JKKJ-22, 19-JKKJ-53); Science and Technology Major Project of Shanxi Province (20181101019).

Corresponding author: LI Deng-hua, Ph. D, Senior engineer. E-mail: yob2846@163.com

1 Introduction

As a kind of famous reinforcing material, carbon fiber has a series of excellent properties such as high specific strength, high specific modulus, high electric

conductivity, high thermal conductivity, low density and high temperature resistance^[1]. Therefore, it has been widely used in the advanced fields of aerospace science and defense technologies, as well as civil fields such as advanced sporting goods and medical

devices^[2]. Nowadays, the carbon fiber industry has developed into a complete and independent new industrial system, and the carbon fiber itself has developed from the original common grade (T300) to medium-strength (T700), high-strength and medium-modulus (T800, T1000), and high-modulus grade (M40, M55, M60) etc^[3].

The complex turbostratic graphite-like structure inside endowed carbon fiber with excellent performance. In terms of element composition, the fiber is mainly composed of carbon element (93 wt% ~99 wt%), which is mainly in sp^2 hybridization state, while sp^3 hybridization carbon also exists at the edge of carbon structures and other defects^[4]. There are also some oxygen, nitrogen, hydrogen and other elements in the fiber, while very little impurity elements such as silicon and calcium could be detected^[5]. Due to the influence of the preparation process and the characteristics of the turbostratic structure, the local structural units have a certain degree of compressive stress^[6]. At the microscopic scale, the carbon layers are arranged in an orderly manner to form the microcrystalline structure, while microvoids are scattered in the non-uniformly distributed microdefects such as the folds and dislocations of carbon layers^[7]. On the mesoscopic scale, the compact crystallites and a few microvoids are closely arranged and thus the so-called microfibril structure is formed, while the transition zone between the fibril is mainly in the amorphous state^[7]. On the micron scale, the radial structure heterogeneity can be observed in most of the stages during the preparation process for almost all of the fibers, anyhow, the so-called skin-core structure can only be found in severe cases^[8]. The above-mentioned structural factors jointly shape the complex structure features and also determine the final performance of carbon fiber. High-performance carbon fiber is believed to have the optimal

combination of the above structural factors, which are obtained by adjusting the production conditions, so as to achieve performance improvement finally^[9].

Carbon fiber has been developed in China for more than 30 years, and a series of major breakthroughs have been made in both scientific work and engineering of this strategic material^[10]. However, research and industrialization of high-performance carbon fibers are still in urgent need, especially when the present excess production capacity in domestic low-end carbon fibers is emerging and the market demand has put forward this product newer and higher requirements. The only way for the development of carbon fiber industry in our country is to break the bottleneck of the production of high-performance fibers and push the research and industrialization level of domestic fibers to a higher level^[11]. However, in order to improve the mechanical properties, it is necessary to firstly obtain the accurate microstructure information and explore the correlation between structure and properties of carbon fibers. In this case, systematic comparative analysis was made in this paper on the crystallites, microvoids, structural inhomogeneity, amorphous structure, internal residual stress, preferred orientation and fractal phenomena of various grades of carbon fibers, based on the current innovative applications of X-ray wide-angle diffraction/small-angle scattering (WAXD/SAXS), Raman spectroscopy and high resolution transmission microscopy (TEM) etc.

2 Experimental

2.1 Samples

The carbon fibers used for this study were all polyacrylonitrile-based fibers derived commercially from Toray Company (Japan) as listed in Table 1.

Table 1 The properties of carbon fibers in this experiment^[12].

Series		Tensile strength /GPa	Tensile modulus /GPa	Elongation at break /%	Bulk density /g cm ⁻³
T series	T300B	3.53	230	1.5	1.76
	T700SC	4.90	230	2.1	1.80
	T800H	5.49	294	1.9	1.81
	T1000G	6.37	294	2.2	1.80
MJ series	M40JB	4.41	377	1.2	1.77
	M55JB	4.02	540	0.8	1.91
	M60JB	3.92	588	0.7	1.93

2.2 Structural characterization

Crystalline parameters were investigated by using an X-ray diffractometer (PANalytical X'Pert PRO, Cu Ka, $\lambda = 0.154\ 0598$ nm, 40 kV, 40 mA) with a fiber specimen attachment. Measurements were made

by performing the equatorial scan, meridian scan, and azimuthal scan at the fixed Bragg position. The step size was about 0.05° and the scan time was set as 30 s per step for the equatorial and meridian scans. The data analysis was processed by MDI Jade 5.0, after

which the structural parameters were calculated according to the Bragg formula and Scherrer equation^[13]. Meanwhile, an X-ray diffraction analysis in the reflection mode was carried out on a D8 Advance powder X-ray diffractometer (Bruker, Cu K α , $\lambda = 0.154\ 06\ \text{nm}$, 40 kV, 40 mA), the experiment and data analysis were conducted according to “JIS R7651-2007 Measurement of lattice parameters and crystallite sizes of carbon”^[9]. Carbon fibers were cut and ground into powder samples, in which silicon powder was added as a reference before the measurement. The scanning step was 0.02° , the residence time was 2 s, and the scanning range was $10^\circ \sim 90^\circ$. The Raman experiment was performed on a Raman spectrometer (Jobin-Yvon, LabRam HR Evolution). The experiment was operated in the continuous scanning mode with a laser beam power of 1 mW and exposure time of 20 s. Spectra were taken for five points at each chosen fiber bundle to confirm the reproducibility of the data. The values of the Raman peak position were determined by a Lorentzian fit with the Peakfit v4.12 software and the structural parameters were calculated with reference to the reports of Li et al^[8].

Small angle X-ray scattering (SAXS) was used to investigate the structure of microvoids of carbon fibers. The experiment was performed using synchrotron radiation as the x-ray source with a long-slit collimation system on the 1W2A beamline in Beijing Synchrotron Radiation Laboratory. The incident x-ray wavelength was 0.154 nm and the scattering angle was $\sim 0^\circ\text{-}3^\circ$. The scattered X-ray intensities were recorded using imagery plate technology and the background scattering of the samples was corrected. Scattering information of both the equatorial and meridian

directions were obtained by rotating the samples for 90° . The data analysis and parameter calculation were based on the reported article by Li et al^[14].

TEM analysis was carried out to obtain the high resolution crystalline morphology of carbon fibers on a FEI Technai G2 F20 transmission electron microscope (accelerating voltage 200 kV).

3 Results and discussion

3.1 Raman spectroscopy

Fig. 1 shows the Raman spectra of the skin and core of carbon fibers. The dotted line indicates the center position of each peak of T300B. As shown in the figure, the *G* band positions of each grade of carbon fibers are significantly different. The *G* band positions of high strength T series fibers are generally around $1\ 587\ \text{cm}^{-1}$, while those of MJ series move rapidly towards lower wavenumbers among which the *G* band of M55JB appears at $1\ 584\ \text{cm}^{-1}$. The *D* band of MJ series also shows a similar phenomenon of moving to lower wavenumbers. Previous studies have shown that *G*, *D* and *G'* band red-shifts are associated with the increase of internal compressive stress, which will be gradually weakened with heat treatment or external tensile stress^[6]. The difference in the degree of red-shift between various series of samples indicates that some of those fibers should have been subjected to a large degree of drawing tension in order to fully release the compression stress during production^[15]. It can be inferred that there is a higher degree of residual stress in T series fibers, while the high orientation and high draft are more significant with the progression of the grades of MJ series.

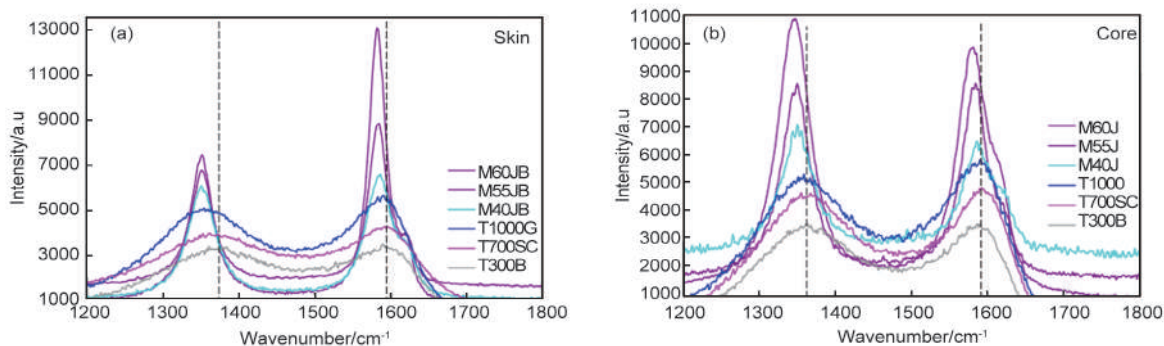


Fig. 1 Raman spectra of (a) the skin and (b) core of carbon fibers.

Fig. 2 shows the FWHM of *D* and *G* band between the skin and core of carbon fibers. As can be seen from the figure, the fibers in the same series do not change much in FWHM, the difference of which between the series is very obvious. It was reported that both the FWHM

of *G* and *D* band decreased sharply with the increase of heat treatment temperature (HTT) before $2\ 000\ ^\circ\text{C}$ and leveled off after $2\ 000\ ^\circ\text{C}$ ^[16]. Thus, it can be concluded that T series fibers might be of similar HTT, while the HTT of MJ series differs with each other.

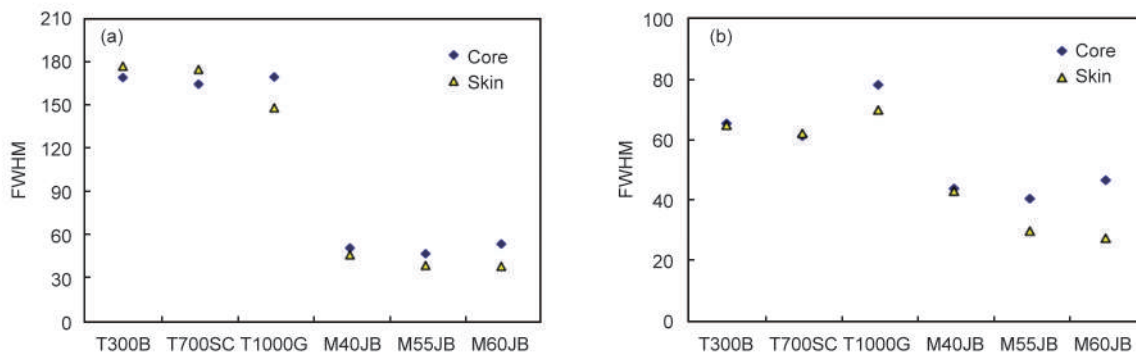


Fig. 2 FWHM of (a) D and (b) G band of the skin and core of carbon fibers.

Fig. 3 shows the graphitization degree between the skin and core of carbon fibers. As can be seen from the figure, the radial structure of T series is relatively homogeneous, while MJ series are obviously heterogeneous. This is consistent with the results reported which have confirmed that graphitization enhances the structural heterogeneity^[8]. The reason may be that, the non-carbon elements diffuse radially from the inside to the outside during graphitization, resulting in an asynchronous recrystallization process between the core and skin, which increases the radial structural inhomogeneity of the fibers. In fact, even the fiber diameters should be changed due to graphitization which in turn enhances the structural heterogeneity of the fibers as reported^[8].

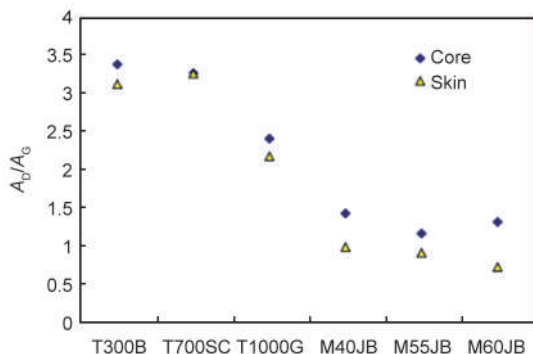


Fig. 3 The graphitization degree of the skin and core of carbon fibers.

Fig. 4 shows the band intensity ratio I_D/I_G of both the skin and core of carbon fibers. As reported, I_D/I_G is a parameter related to the crystalline structure and has an approximate inverse correlation with the crystallite size of carbon fibers^[17]. It can be concluded from all above that the crystalline structure is improved from T series to MJ series, but the improvement is asynchronous in general between the skin and the core of the fibers. In summary, most of the Raman results including FWHM, band positions, values

of I_D/I_G , and graphitization degree tend to reflect a fact that the fibers are enhanced in the crystalline structure but exacerbated in the radial structural inhomogeneity of the fibers.

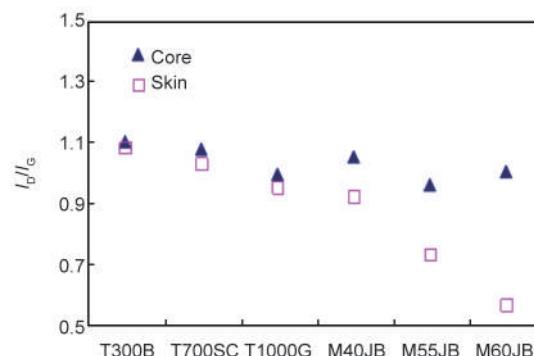


Fig. 4 The I_D/I_G values of the skin and core of carbon fibers.

3.2 X-ray diffraction

X-ray diffraction can help to further explore the crystalline structure of carbon fibers. Fig. 5 shows the dimensions of the crystallites of various grades of carbon fibers. It can be seen from the figure that the stacking thickness L_c of MJ series fibers are greatly improved compared with those of T series, regardless of the data received on reflection mode or transmission mode. There is no significant difference between T300B and T700SC in L_c value, while the stacking thickness of T1000G is slightly larger than that of the former. Meanwhile, it can be clearly observed that the values of L_c of MJ series have increased gradually with the progression of the fiber grade. This remarkable improvement in crystalline structure is believed to be attributed to the heat treatment and hot-stretching during the high temperature graphitization.

An increasing trend can be observed also in another two parameters namely the dimensions of the crystallites $L_{a\perp}$ and $L_{a\parallel}$, but their increasing amplitudes are of great difference. For $L_{a\parallel}$, there is little difference between T series fibers but a significant

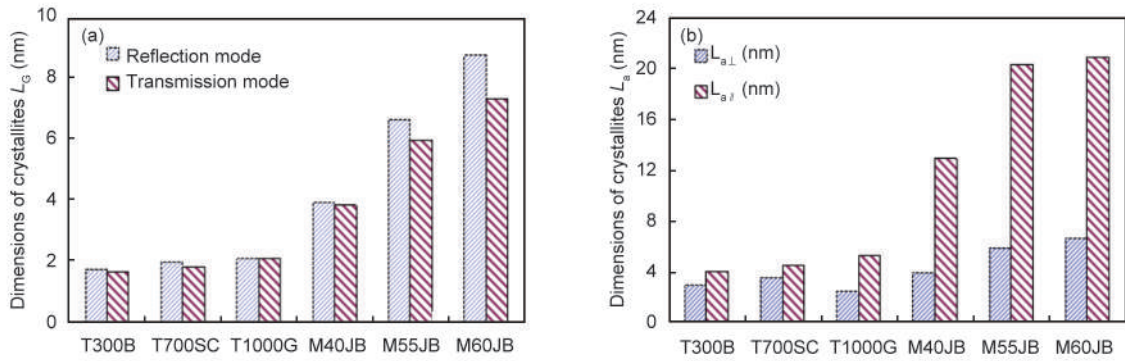


Fig. 5 The crystallite dimensions (L_c and L_a) s of carbon fibers.

gradual increase between MJ series. Moreover, $L_{a\parallel}$ of MJ series is generally greatly improved than that of T series, which is similar to the change on stacking thickness L_c . The dimensional change of $L_{a\perp}$ is, somehow, not so obvious. Firstly, the value difference of $L_{a\perp}$ between T series is relatively small, among which T1000G even shows a lower $L_{a\perp}$ than T300B and T700SC. Secondly, the value of M40JB

also does not increase significantly compared with that of T series. The difference in the changes of $L_{a\perp}$ and $L_{a\parallel}$ may indicate that, the (002) plane of L_a has an in-plane growth difference between the fiber axis and its normal direction during graphitization, which may also be attributed to the drafting effect applied along the axis.

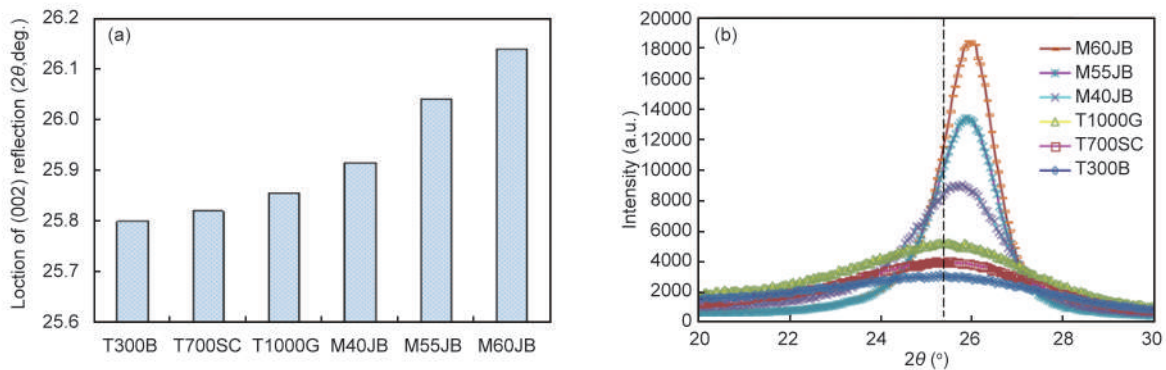


Fig. 6 (a) Peak positions of (002) reflection under reflection mode and (b) transmission mode of XRD.

Fig. 6 shows the peak positions of (002) reflection under reflection mode and transmission mode of XRD. As can be seen from the figure, under either one of the two test modes, the positions of carbon (002) reflection are observed to move from $\sim 25.8^\circ$ to $\sim 26.1^\circ$ with the progression of the fiber grade. The phenomenon should be attributed to the transformation of the carbon lattice caused by the thermal-induced release of internal compressive stress. According to the Bragg formula the interlayer spacing $d(002)$ is inversely correlated with $\sin\theta$ under a certain incident X-ray wavelength^[13]. Therefore, the position migration of (002) reflection is mainly related to the change on interlayer spacing. In other words, with the improvement of the crystallite structure, the position of (002) reflection moves to a higher angle.

Fig. 7 shows the interlayer spacings of carbon fibers obtained from the reflection mode XRD. It is

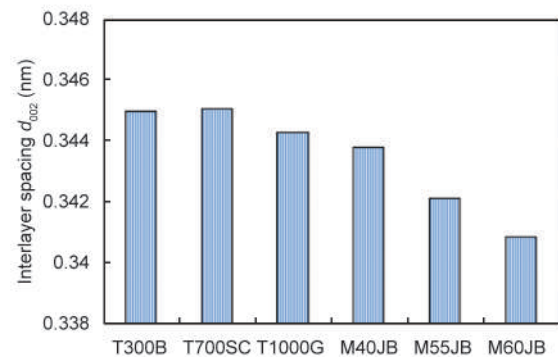


Fig. 7 Interlayer spacings of various grades of carbon fibers.

clear that the value of interlayer spacings generally shows a trend of a gradual decrease with the progression of the fiber grade. Among them, the spacing changing between T series fibers is rather small. T300B and T700SC share a similar larger d_{002} among

all the T series due to their disordered and curled crystalline stacking, while T1000G decreases to 0.344 3 nm finally. The interlayer spacing of MJ series fibers, on the other hand, decreases rapidly reaching about 0.341 nm at one time. In essence, the decrease of interlayer spacing is related to the high temperature treatment, the gradual escape of non-carbon heteroatoms and the orderly rearrangement of the random graphite layers during carbonization and graphitization^[18].

Fig. 8 shows the orientation angle of various grades of carbon fibers. As shown in the figure, the crystallite orientation is improved as a whole and the orientation angle is gradually decreased with the progression of the fiber grade. There is still no significant difference between the T series fibers, and their orientation angle varies from 35° to 32°. Meanwhile, M40JB shows a rapid decrease to 21.9°, and M55JB and M60JB are further oriented to reach 12.3°.

From the above, we find each grade of fibers have a certain level of interlayer spacing, preferred orientation, crystalline dimensions, etc. Their differences on the crystalline structure reflect the specific effect of draft and heat treatment during carbonization or graphitization. Furthermore, the crystallites should experience a mutually collaborative evolution in the aspect of interlayer spacing, preferred orientation, crystalline dimensions, etc., which results in such a strict order of the crystalline structure.

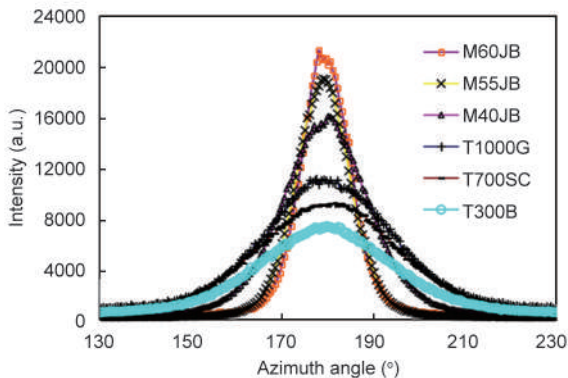


Fig. 8 Preferred orientation of various grades of carbon fibers.

3.3 Small angle X-ray scattering

SAXS is a powerful tool in the study of the interior closed microvoids of carbon fibers. As shown in Fig. 9, the microvoids are ellipsoid, which are about 1 nm at the short axis and 3 nm at the long axis for the T series fibers, among which no obvious difference can be observed. The voids' dimensions of MJ series are rather large, and the dimensions of both axes are gradually increased with the progression of the fiber grade. The increasing trend on the voids' dimensions is closely

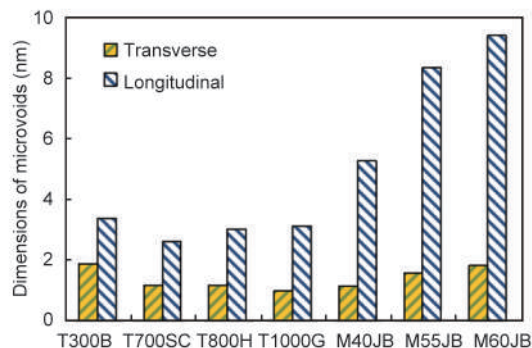


Fig. 9 The dimensions of the microvoids of various grades of carbon fibers.

related to the heat treatment process. During the graphitization, both the density and size of crystallites increase significantly after the orderly rearrangement of graphitic layers, which may indirectly enlarge the dimensions of the microvoids. Meanwhile, the microvoids also show an asynchronous change between the fiber axis and its normal direction liking the crystallites do during the graphitization, which should also be attributed to the hot-stretching applied along the fiber axis.

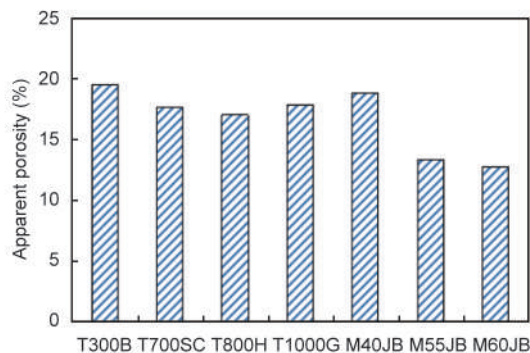


Fig. 10 Apparent porosity of various grades of carbon fibers.

Fig. 10 shows the apparent porosity of various grades of carbon fibers. The porosity of T series fibers and M40JB is maintained at a high level (17.0%-20.0%), while that of M55JB and M60JB is relatively low, between 13.0%-14.0%. Here are some ideas based on the data. Firstly, the apparent porosity is mainly related to the bulk density and interlayer spacing, the two aspects of T series are generally at a low level. The increase on apparent porosity indirectly reflects that the crystalline areas in MJ series are condensed in density and enlarged in dimensions compared with that of T series. Secondly, given both the increased porosity and voids' dimensions, the total number of voids should sharply decline for MJ series. Graphitization promotes the orderly stacking of graphitic layers

and integrates the small crystallites into large crystalline regions. In this case, some voids within the crystalline regions will be naturally annihilated, while the others at the edges or the junctions between the adjacent crystalline regions appear to be increased in dimension. However, compared with the annihilated microvoids, the enlarged voids are very rare in number and occupy only a limited space.

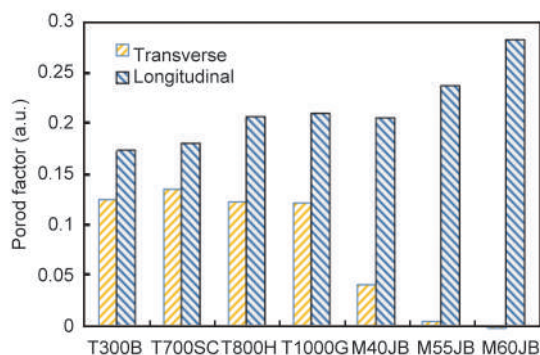


Fig. 11 Porod factors of various grades of carbon fibers.

Porod coefficient is a parameter related to the local electron density fluctuation of the scatterers and the conditions of the internal interface^[19]. For an ideal two-phase-system with sharp interfacial transition and uniform electron density distribution, Porod coefficient approaches zero. When the local structure is of disorder and the electron density becomes inhomogeneous within any one of the phases, the coefficient will increase. When the system has a diffuse interface transition, the coefficient decreases^[20]. The microstructure of carbon fibers is very complex, which may be affected by both the above two factors^[21]. The data of this study shows that the axial Porod coefficient increases gradually with the progression of the fiber grade, while the radial Porod coefficient decreases gradually. In our previous study, the factors are observed to decrease in both axes during an intermittent graphitization without stretching. Therefore, we believe in this study hot-stretching may have played a significant role in the anisotropic changing of Porod factors. However, the precise rules of the influence still need to be further explored.

In many recent articles on the small-angle scattering of carbon fibers, the results have been interpreted in terms of fractal structures^[21]. In SAXS methodology, in order to quantitatively describe the self-similarity of a system, the concept of Hausdorff dimension (i. e. fractal dimension) is introduced to characterize the quantitative properties of the self-similar system^[22]. Among them, surface fractal refers to the irregular self-similar surface of a dense object, and the

surface fractal dimension D_s represents the degree of irregularity or roughness of the surface^[23, 24]. $2 \leq D_s \leq 3$, the larger the value of D_s , the rougher the surface. $D_s = 2$ stands for smooth surface, while $D_s = 3$ indicates that the surface is so complex that it fills the space and becomes an entity^[25].

As can be seen from Fig. 12, the fractal dimension shows a trend of slight increase with the progression of the fiber grade within T series. Such a trend reflects that the stacking of graphite layers has a characteristic of being between a plane and a bulk structure that is biased toward the plane, i. e. being between two-dimensional and three-dimensional and close to the two dimensional plane. The results also show that the fractal dimension gradually increases with the increase of tensile strength of carbon fibers. As reported, the fractal dimension tends to influence the propagating process of the microstress and cracks during tensile deformation and hence has a nonlinear relationship with tensile strength. When the graphitic layers are arranged at a three-dimensional condition, there would be many overlappings and even winding parts between the layers. The graphitic layers thus are difficult to slip from the adjacent layers and the applied stress in this case can be fully transferred to the adjacent layers during the tensile deformation. Furthermore, there is still the possibility of incomplete release of compressive stress in the curled layers, and the applied tensile stress to deform the fiber must first offset the compressive stress within the layers, which in turn increase the measured tensile strength.

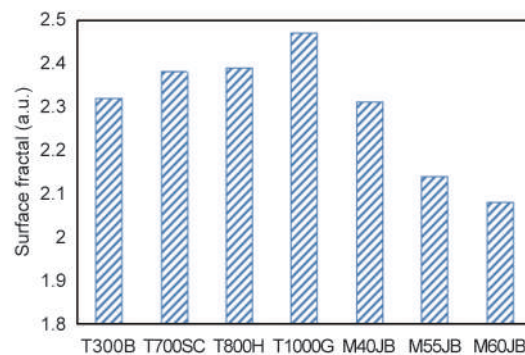


Fig. 12 The surface fractal dimensions of various grades of carbon fibers.

For MJ series fibers, the surface fractal dimension approaches 2, indicating that the graphitic layers are getting closer to the two-dimensional smooth surface. Because of the lack of interlaminar binding force and the development of microvoids into larger size, the tensile fracture of the fibers of high crystallinity shows a feature of hardness and brittleness, of

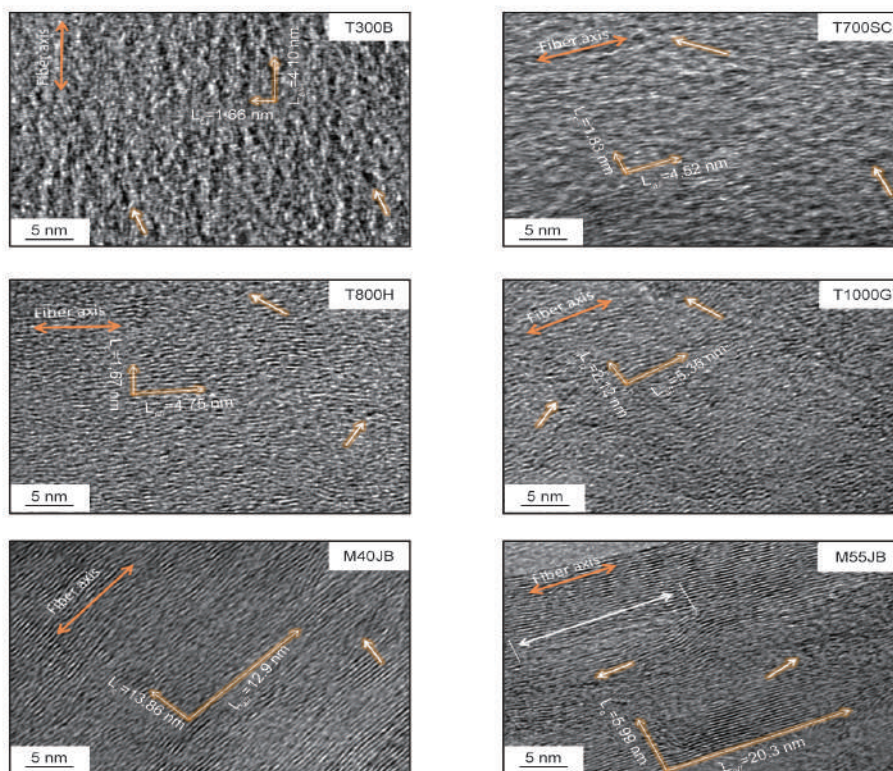


Fig. 13 TEM images of various grades of carbon fibers.

which the strength is decreased to different degrees compared with that of T series fibers. However, due to the same reason the strain degree of MJ series fibers is smaller under the applied stress, and thus the modulus is significantly higher than that of T series fibers.

3.4 Transmission electron microscopy

Fig. 13 are the TEM images of the axial crystalline structure of each grade of carbon fibers. According to the images, the crystallites of T300B and T700SC are relatively smaller, with larger interlayer spacings and ambiguous orientation along the axial direction. The graphitic layers are all curled and messy in pattern and present a shape of discontinuity or semi-continuity. The crystalline structures of T800H and T1000G are significantly improved in both dimension and texture, while the graphitic layers are still curved and do not extend sufficiently. The curled graphitic texture has been reported to evolve from the heat-resistant trapezoidal structure in the pre-oxidation stage to the layered structure by the heat treatment and drawing tension during carbonization stage^[26].

The TEM images are consistent with the results of residual compression stress obtained by Raman spectroscopy. In M40JB and M55JB, the graphitic layers are extended to some extent in morphology, and the residual stress within the crystallites is almost released. Meanwhile, the crystallites grow in all directions with

enhanced preferred orientation along the fiber axis, and the graphitic layers become continuous in two-dimension and compact in three-dimension. The double arrow in M55JB indicates the connecting part of the two large crystalline regions, whose morphology is similar to the splitting of crystallites. The splitting forms a big void with a length at about 12 nm which is very close to the voids' dimensions by SAXS. The single arrow indicates the disordered structure beside the crystalline regions, which further indicates the complex structure featured by the coexistence of crystallites and voids, the curl of graphitic layers and the accumulation of stress. In addition, the results of electron density fluctuation and fractal structure mentioned above can also be verified by the stacking state of microcrystallites in the image. All in all, the TEM images give an intuitive sense that the crystallites are enlarged in dimension and better-arranged in texture, voids are enlarged in dimension and reduced in quantity with the progression of the fiber grade.

4 Conclusions

Residual stress and fractal: XRD and Raman spectra show that there are different degrees of residual compressive stress in carbon fibers. In total, the residual stress of MJ series fibers is slighter than that of T series, of which the TEM images show a typical fea-

ture of the stacking of small curled graphitic layers. With the progression of the fiber grade, the fractal dimension of T series tends to increase, corresponding to their increasing structural complexity, bulk density and radial density fluctuation. For MJ series fibers, the surface fractal dimension approaches 2, indicating that their graphitic layers are getting closer to a smooth surface.

Crystallite: The crystalline structure of MJ series is generally improved compared with that of T series. There is no significant difference between T300B and T700SC in crystalline dimensions, while the crystalline size of T1000G is slightly larger than those of T300B and T700SC. Meanwhile, the crystalline dimensions gradually increase for M40JB, M55JB and M60JB. Nevertheless, the changing trends of interlayer spacing and angle of orientation are generally observed to be opposite to that of crystalline dimensions which further confirm the improvement of crystalline structure.

Microvoid: There is no obvious difference between T series in void's dimension, among which the long axis is about 3 nm, and the short axis is less than 1 nm. The void's size of MJ series becomes larger gradually, whose sizes in the long and short axis all show an increasing trend with the progression of the fiber grade. The apparent porosities of T series fibers and M40JB are maintained at a high level at 17.0%-20.0%, while those of M55JB and M60JB are relatively low, at 13.0%-14.0%.

Graphitization degree and structural heterogeneity: The difference between T300B and T700SC in graphitization degree is not so significant, and also far lower than that between MJ series. The graphitization degree of T1000G is between the two series fibers mentioned above. The radial structure heterogeneity of the fibers is characterized by a large core area and a very thin skin, and this feature is particularly obvious with the progression of the fiber grade of MJ series.

References

- [1] Ruland W. Carbon fibers [J]. *Adv Mater*, 1990, 2(11): 528-536.
- [2] Renhofer H, Loidl D, Puchegger S, et al. Structural development of PAN-based carbon fibers studied by in situ X-ray scattering at high temperatures under load [J]. *Carbon*, 2010, 48(4): 964-971.
- [3] Diefendorf R J, Tokarsky E. High-performance carbon fibers [J]. *Polymer Engineering & Science*, 1975, 15(3): 150-159.
- [4] Guigon M, Oberlin A, Desarmot G. Microtexture and structure of some high tensile strength, PAN - base carbon fibres [J]. *Fibre Sci Technol*, 1984, 20(1): 55-72.
- [5] Johnson D J, Tyson C N. The fine structure of graphitized fibres [J]. *J Phys D Appl Phys*, 1969, 2(6): 787.
- [6] Li D H, Lu C X, Wu G P, et al. Heat-induced internal strain relaxation and its effect on the microstructure of polyacrylonitrile-based carbon fiber [J]. *J Mater Sci Technol*, 2014, 30(10): 1051-1058.
- [7] Li D, Lu C, Du S, et al. Structural features of various kinds of carbon fibers as determined by small-angle X-ray scattering [J]. *Appl Phys A*, 2016, 122(11): 956.
- [8] Li D H, Lu C X, Wu G P, et al. Structural heterogeneity and its influence on the tensile fracture of PAN-based carbon fibers [J]. *RSC Adv*, 2014, 4(105): 60648-60651.
- [9] Rahaman M S A, Ismail A F, Mustafa A. A review of heat treatment on polyacrylonitrile fiber [J]. *Polymer Degradation and Stability*, 2007, 92(8): 1421-1432.
- [10] Zhang M, Ogale A A. Carbon fibers from dry-spinning of acetylated softwood kraft lignin [J]. *Carbon*, 2014, 69(0): 626-629.
- [11] Li C, Xian G. Experimental and modeling study of the evolution of mechanical properties of PAN-based carbon fibers at elevated temperatures [J]. *Materials*, 2019, 12(5): 724.
- [12] Li W, Long D H, Miyawaki J, et al. Structural features of polyacrylonitrile-based carbon fibers [J]. *J Mater Sci*, 2012, 47(2): 919-928.
- [13] Liu F, Wang H, Xue L, et al. Effect of microstructure on the mechanical properties of PAN-based carbon fibers during high-temperature graphitization [J]. *J Mater Sci*, 2008, 43(12): 4316-4322.
- [14] Li D H, Lu C X, Wu G P, et al. Structural evolution during the graphitization of polyacrylonitrile-based carbon fiber as revealed by small-angle X-ray scattering [J]. *J Appl Cryst*, 2014, 47(6): 1809-1818.
- [15] Guigon M, Oberlin A. Heat-treatment of high tensile strength PAN-based carbon fibres: Microtexture, structure and mechanical properties [J]. *Fibre Sci Technol*, 1986, 27(1): 1-23.
- [16] Dresselhaus M, Dresselhaus G, Pimenta M, et al. Raman scattering in carbon materials [J]. *Analytical applications of Raman spectroscopy*, 1999, 367-434.
- [17] Mallet-Ladeira P, Puech P, Toulouse C, et al. A Raman study to obtain crystallite size of carbon materials: A better alternative to the Tuinstra-Koenig law [J]. *Carbon*, 2014, 80(1): 629-639.
- [18] Johnson J W, Marjoram J R, Rose P G. Stress graphitization of polyacrylonitrile based carbon fibre [J]. *Nature*, 1969, 221(5178): 357-368.
- [19] Ruland W. Small-angle scattering of two-phase Systems: Determination and Significance of Systematic Deviations from Porod's Law [J]. *J Appl Cryst*, 1971, 4(1): 70-73.
- [20] Cohaut N, Guet J M, Diduszko R, et al. SAXS investigations on the porosity of pitch based carbon fibres [J]. *Carbon*, 1996, 34(5): 674-6.
- [21] Ruland W. Apparent fractal dimensions obtained from small-angle scattering of carbon materials [J]. *Carbon*, 2001, 39(2): 323-334.
- [22] Schmidt P. Small-angle scattering studies of disordered, porous and fractal systems [J]. *J Appl Cryst*, 1991, 24(5): 414-435.
- [23] Bale H D, Schmidt P W. Small-angle X-ray-scattering investigation of submicroscopic porosity with fractal properties [J]. *Physical Review Letters*, 1984, 53(6): 596-609.
- [24] Teixema J. Small-angle scattering by fractal systems [J]. *Journal of Applied Crystallography*, 1988, 21(6): 781-785.
- [25] Kaneko K, Sato M, Suzuki T, et al. Surface fractal dimension of microporous carbon fibres by nitrogen adsorption [J]. *J Chem Soc Faraday T*, 1991, 87(1): 179-184.
- [26] Johnson D J, Tomizuka I, Watanabe O. The fine structure of pitch-based carbon fibres [J]. *Carbon*, 1975, 13(6): 529-534.